`

Engineering anaerobic fungal-bacterial consortia for medium-chain fatty acid production from lignocellulosic biomass

Byung-Chul R. Kim[1], Elaina M. Blair[2], Joel P. Howard[1], Ian M. Gois[1], Robert Flick[1], Stephen Mondo[3], Jasmyn Pangilinan[3], Anna Lipzen[3], Jie Guo[3], Hope Hundley[3], Raymond Lee[3], Jayson Talag[4], Victoria Bunting[4], Shanmugam Rajasekar[4], Kerrie Barry[3], Igor V. Grigoriev[3,5], Michelle A. O'Malley[2,6], Christopher E. Lawson[1]*

[1]Department of Chemical Engineering & Applied Chemistry, University of Toronto, Toronto, ON, Canada

[2]Department of Chemical Engineering, University of California, Santa Barbara, CA, USA

[3]US Department of Energy Joint Genome Institute, Lawrence Berkeley National Laboratory, Berkeley, CA, USA

[4]Arizona Genomics Institute, School of Plant Sciences, University of Arizona, Tucson, AZ, USA

[5]Department of Plant and Microbial Biology, University of California Berkeley, Berkeley, CA, USA

[6]Department of Bioengineering, University of California, Santa Barbara, CA, USA

*Correspondence should be addressed to: Christopher E. Lawson E-mail: chris.lawson@utoronto.ca

`

Abstract

Anaerobic fermentation of lignocellulosic biomass offers a cost-effective route for sustainable biomanufacturing, yet constructing synthetic consortia for targeted bioproduction remains challenging. Inspired by herbivore rumen microbiome, we engineered bottom-up anaerobic fungal-bacterial consortia for direct conversion of lignocellulose to medium-chain fatty acids (MCFAs). Initial screening experiment identified a newly isolated fungal strain, *Neocallimastix* sp. FC1, in co-culture with the bacterial strain *Megasphaera hexanoica*, as an optimal co-culture pair, achieving 21.0 % (carbon-to-carbon basis) lignocellulose-to-MCFAs yield. Lactate, the main fermentation product of *Neocallimastix* sp. FC1 and primary substrate for *M. hexanoica*, was undetectable in co-culture suggesting tight cross-feeding. This triggered upregulation of reverse β-oxidation pathway enzymes in *M. hexanoica*, favoring the production of MCFAs (hexanoate and octanoate) over butyrate. These results suggest that securing high-performing lactate-producing fungi, while maintaining low lactate levels, could be a promising strategy to maximize lignocellulose-to-MCFA conversion. Technoeconomic analysis further supported the process's economic feasibility and delineated the cost-yield ranges required for profitable implementation.

`

Main

Bioconversion of lignocellulosic biomass to fuels and commodity chemicals holds significant potential as a sustainable alternative to traditional petroleum-based processes due to the low purchase cost and renewable production capacity of biomass feedstocks[1,2]. Microbial systems that combine multiple biological functions offer promising routes for low-cost biomass processing, particularly when integrated into a single step, as in consolidated bioprocessing (CBP)[2,3]. However, integrating entire reaction cascades into a single microbial host can impose a substantial metabolic burden, thereby limiting the overall system productivity[3,4]. Anaerobic microbiomes provide an alternative model based on metabolic division of labor, enabling conversion of complex feedstocks at efficiencies near thermodynamic limits[5]. Nonetheless, microbiomes face inherent limitations, including low productivity, product diversity, and process control. To address these limitations while harnessing the benefits of metabolic division of labor, synthetic consortia offer a promising strategy by enabling rational assembly of complementary microbial functions that can be more precisely controlled.

Herbivore rumen microbiomes are exemplary cases of metabolic division of labor and have co-evolved with their hosts to convert lignocellulose into volatile fatty acids[6]. Herbivore rumen microbiomes contain diverse archaea, bacteria, and eukaryotic microorganisms, where anaerobic fungi have been identified as key candidates for lignocellulose degradation, a major bottleneck of lignocellulose utilization[6–8]. Indeed, anaerobic fungi are known to encode the largest number of biomass-degrading enzymes found in nature[7], and are responsible for releasing up to 50 % of the fermentable sugars from ingested plant matter while constituting only a very small percentage of the gut microbiota in their hosts (7-9 %)[8,9]. Additionally, anaerobic fungi possess unique root-like morphologies (i.e., rhizoids) and enzyme complexes

`

(i.e., cellulosomes) which allows them to penetrate the intricate plant cell structure and intrude upon polysaccharides, obviating the need for feedstock pre-treatment, which is a common and costly step in bioprocesses that utilize lignocellulosic biomass feedstocks[7,10,11].

Anaerobic gut fungi exhibit mixed acid fermentation, producing principally formic, acetic, and lactic acids, as well as ethanol, hydrogen, and carbon dioxide[12]. These metabolites can be further upgraded into a range of value-added products by co-culturing anaerobic fungi with a microbial partner that performs a secondary fermentation, such as methane[13–15], butyrate and butanol[16], ethyl acetate, 2-phenyl ethanol, isoamyl alcohol[17], and medium-chain fatty acids (MCFAs)[18]. Among these processes, MCFA production through microbial chain elongation using the reverse β-oxidation (RBO) pathway has outstanding potential as a versatile future refinery platform[19]. MCFAs are high-value commodity chemicals, feedstocks for biofuels in heavy-duty and aviation applications[2,20], and precursors of alcohols, esters, methyl ketones[19], and diols[21]. Moreover, MCFAs can be separated from the fermentation broth through extraction owing to their relatively higher hydrophobicity[20,22].

Inspired by the herbivore rumen microbiome, this study aims to construct synthetic fungal-bacterial consortia that can directly convert lignocellulosic biomass into MCFAs (Fig. 1). To achieve this, a bottom-up microbiome engineering approach was applied, based on assembling fungal and bacterial isolates that perform lignocellulose conversion to lactate, and lactate conversion to MCFAs via chain elongation, respectively. To secure high-performing candidates, a new lactate-producing fungal isolate (*Neocallimastix* sp. FC1) was obtained. The co-culture combination with the highest MCFA productivity was identified through screening of three fungal and seven bacterial isolates and was found to consist of *Neocallimastix* sp. FC1 and *Megasphaera hexanoica*. Interestingly, co-cultures produced higher yields of the more desirable hexanoic and octanoic acid compared to monocultures.

`

Kinetic and proteomic analyses revealed that this shift was driven by lactate-scarcity resulting from tight cross-feeding, suggesting that maintaining low lactate levels while sustaining high flux could serve as a key strategy for process optimization. Lastly, technoeconomic analysis pinpointed medium cost, solids loading, and MCFA yield as primary barriers of economic viability, which can be used to guide commercial implementation of the lignocellulose-to-MCFA platform.

Results

Co-culture screening identifies optimal fungal-bacterial partners for MCFAs production

To identify optimal co-cultures for lignocellulose conversion into MCFAs, we first isolated a high-lactate-producing fungal strain, *Neocallimastix* sp. FC1, from a lignocellulose-degrading enrichment culture derived from a cow fecal sample[23]. We sequenced and annotated its genome to support systems-level analysis, which is summarized in Supplementary Table 1. Subsequently, we selected promising strains of anaerobic fungi and chain elongating bacteria based on previously reported biomass degradation and lactate utilization capabilities, respectively, and the availability of genome sequence data to enable systems-level investigation of microbial interactions. This resulted in 3 anaerobic fungal isolates (*Neocallimastix* sp. FC1, *Neocallimastix camerooni* var. *constans*, and *Caecomyces churrovis*) and 7 lactate-utilizing chain elongating isolates (*Caproicibacter fermentans*, *Caproiciproducens* sp. 7D4C2, *Clostridium luticellarii*, *Pseudramibacter alactolyticus*, *Megasphaera cerevisiae*, *Megasphaera elsdenii*, and *Megasphaera hexanoic*a) that were further screened in monoculture and co-culture to evaluate bioconversion performance (Supplementary Fig. 1, 2).

The selected fungal and bacterial isolates were first tested in monoculture to assess

`

their ability to carry out lignocellulose degradation or chain elongation in a chemically defined M2 medium with 10 g/L (1%) milled reed canary grass (1 mm). Fungal monocultures were incubated for seven days, as determined by a preliminary kinetic experiment (Supplementary Fig. 3), and 100 mg/L chloramphenicol was supplemented. All three isolates actively degraded reed canary grass, and produced formate, acetate, and lactate as major fermentation products (Fig. 2a). In our lignocellulose-to-MCFAs conversion process, lactate acts as a central intermediate in fungal-bacterial cross-feeding, making its titer the key parameter for evaluating the function of fungal isolates. *N*. sp. FC1, a newly isolated fungal strain from this study, exhibited the highest lactate titer, reaching 1.46±0.22 g/L, which was about twice as high as that of *N. camerooni* var. *constans* and *Caecomyces churrovis* (0.76±0.04 and 0.61±0.18 g/L, respectively). The lignocellulose-to-product conversion yield of *N*. sp. FC1 was 49.3 % (carbon-to-carbon basis, see Materials and Methods) after seven days of fermentation and reached 58.1 % after 21 days.

The growth of bacterial monocultures was subsequently assessed in the same medium (i.e., M2 medium with reed canary grass) without chloramphenicol but supplemented with yeast extract, lactate, and acetate (1, 1.8, and 2.6 g/L, respectively). Yeast extract was added to support bacterial growth, and the concentrations of lactate and acetate were set to match those produced by *N*. sp. FC1 in monoculture. *M. elsdenii*, *M. hexanoica*, and *P. alactolyticus* produced butyrate and hexanoate, while the four other species didn't show any clear evidence of growth (Fig. 2b). Lactate was completely consumed by all three active strains, whereas acetate utilization differed across strains. *M. elsdenii* and *M. hexanoica* exhibited net consumption of acetate, but *P. alactolyticus* did not. Furthermore, three sister species, *M. cerevisiae*, *M. elsdenii*, and *M. hexanoica* showed diverging results. While *M. cerevisiae* didn't grow under the condition tested, *M. elsdenii* and *M. hexanoica* showed the highest titer of butyrate (1.29±0.05 g/L) and hexanoate (0.68±0.02 g/L), respectively, among seven chain

`

elongators.

Optimal fungal-bacterial partners for MCFA production were determined by screening co-culture combinations cultivated in M2 medium supplemented with reed canary grass and yeast extract (10 and 1 g/L, respectively) (Fig. 2c). The co-culture composed of the top-performing isolates from the fungal and bacterial monoculture screenings, *N*. sp. FC1 and *M. hexanoica*, exhibited the highest lignocellulose-to-MCFAs conversion efficiency (21.0 % carbon-to-carbon yield, see Materials and Methods), and was the only culture that produced octanoate across all screening conditions. The other two bacterial isolates that thrived in the monoculture experiments, *M. elsdenii* and *P. alactolyticus*, also demonstrated robust growth in co-culture. While co-culture containing *M. elsdenii* primarily produced butyrate, the co-culture containing *P. alactolyticus* produced higher levels of hexaonate. Surprisingly, *Caproiciproducens* sp. 7D4C2, *Caproicibacter fermentens*, and *M. cerevisiae*, which didn't grow in monoculture, grew in co-culture. This may reflect fungal-bacterial interactions beyond lactate cross-feeding, although the exact mechanism requires further investigation.

Interestingly, chain elongators (i.e., *M. elsdenii*, *M. hexanoica*, and *P. alactolyticus*) showed higher MCFA specificity when co-cultivated with *N*. sp. FC1 compared to monoculture (Fig. 2b, 2c). The average number of RBO cycles involved in product formation was consistently higher in co-cultures with *N*. sp. FC1 than in monocultures (Fig. 2d). The increase was more substantial in strains that exhibited higher MCFA specificity in monoculture. To assess whether the enhanced MCFA specificity in co-culture could be attributed to differences in fungal-mediated degradation, we conducted a carbon mass balance analysis comparing monoculture of *N*. sp. FC1 and its co-culture systems with *M. hexanoica* (Fig. 2e). This revealed that solid-carbon reduction was lower in the co-culture (25.5 %) compared to the monoculture (39.5 %), likely due to the product (i.e., MCFAs) inhibition on

`

N. sp. FC1. Nevertheless, higher MCFA production from a smaller amount of degraded carbon indicated that co-cultivation has higher carbon conversion efficiency toward MCFAs.

Proteomic analysis highlights fungal-bacterial cross-feeding and metabolic shift toward medium-chain fatty acids production in co-culture

To better understand the mechanistic basis of metabolite cross-feeding and its link to improved MCFA production in co-culture, we performed comparative proteomic analysis of monoculture and co-culture systems (Fig. 3a, Supplementary dataset 1). This allowed us to establish functional baselines for each organism. In *N*. sp. FC1, malic enzyme, pyruvate formate lyase, and xylose isomerase (Enzymes 17, 18, and 7 in Fig. 3a, respectively) were the most abundant proteins (Supplementary Table 2). Malic enzyme and pyruvate formate lyase are key enzymes of the hydrogenosome, a mitochondria-like organelle of anaerobic fungi specialized in producing ATP and H_2[12]. This finding is consistent with the observed active production of acetate and formate (Fig. 2a). The abundance of xylose isomerases also highlights the potential of anaerobic fungi as a key biocatalyst for lignocellulose-based refineries, given that the lack of efficient industrial xylose-fermenting microbes limits hemicellulose utilization[24,25]. In the *M. hexanoica*, electron transfer flavoprotein, enoyl-CoA hydratase, and pyruvate:ferredoxin oxidoreductase (Enzymes 32, 31, and 28 in Fig. 3a, respectively), all key enzymes for chain elongation, were the most abundant proteins (Supplementary Table 2), underscoring the metabolic specialization of this strain.

Although this study analyzed only intracellular proteins, a diverse set of CAZymes was identified in *N*. sp. FC1 (Fig. 3b). A broad array of endoglucanases, exoglucanases, and β-glucosidases (e.g., GH1, GH3, GH5, GH6, GH9, GH13, GH45, and GH48), as well as hemicellulases (e.g., GH10, GH11, GH43, and CE1), were identified (Supplementary dataset

`

1). Most of the CAZymes contained carbohydrate-binding domains (CBMs), such as CBM10, CBM6, and CBM13, which are known to enhance substrate affinity and synergistic catalysis[26]. In anaerobic fungi, the frequent occurrence of CBM10 is particularly noteworthy, as it may also function as a dockerin-like domain that anchors catalytic subunits to scaffoldins[27]. Indeed, a scaffoldin protein was detected, strongly supporting the presence of a cellulosome-like enzymatic complex in *N*. sp. FC1. This, together with the presence of proteins harboring diverse domain combinations, points to a system that combines broad catalytic capability with specificity toward particular substrates (Fig. 3b, Supplementary dataset 1). For example, a single protein sequence contained both GH3 and GH6 domains along with three CBM10 domains, while another protein sequence included GH43_16 together with three distinct CBM domains (CBM6, CBM13, and CBM10). GH43_29 was also detected in four tandem repeats, together with two CBM10 domains. Together, these features may facilitate efficient lignocellulose breakdown and suggest an important role for *N*. sp. FC1 in metabolic exchange within the co-culture.

Metabolite cross-feeding between *N*. sp. FC1 and *M. hexanoica* under co-culture cultivation was predominantly based on D-lactate. *N*. sp. FC1 solely produced D-lactate but not L-lactate, in agreement with genomic evidence showing the presence of a D-lactate dehydrogenase gene and not a gene for L-lactate dehydrogenase. However, the abundance of lactate racemase and L-lactate dehydrogenase in *M. hexanoica* did not differ significantly between monoculture and co-culture (Fig. 3a, Supplementary Table 2). The absence of sugar transporters (e.g., PTS subunits IIABC) and metabolic enzymes (e.g., hexokinase, xylose isomerase) in *M. hexanoica* proteome, together with undetectable sugar levels in fungal monoculture, suggests minimal sugar-mediated cross-feeding. Interestingly, enzymes involved in riboflavin biosynthesis (6,7-dimethyl-8-ribityllumazine synthase, Supplementary Table 2) were downregulated in *M. hexanoica* under co-culture, suggesting potential cross-

`

feeding of trace micronutrients. Such micronutrient transfer may have facilitated the growth of strains that failed to grow in monoculture (*Caproiciproducens* sp. 7D4C2, *Caproicibacter fermentens*, and *M. cerevisiae*; Fig. 2b, 2c) under co-culture, pointing to fungal-bacterial interactions beyond lactate cross-feeding. In addition, *M. hexanoica* proteins related to nitrogen metabolism exhibited marked shifts in abundance under co-culture, suggesting restricted access to nitrogen source due to competition with the fungal partner (Supplementary Note 1, Supplementary Table 2).

Differential proteomic analysis between monoculture and co-culture conditions revealed that the enhanced production of hexanoate and octanoate over butyrate in co-culture was driven by changes in the bacterial proteome. While *N*. sp. FC1 proteome showed no statistically significant differences, *M. hexanoica* exhibited a marked upregulation of chain elongation pathways under co-culture. All enzymes involved in the RBO cycle were upregulated, except acetyl-CoA C-acetyltransferase (Enzyme 29 in Fig. 3a) which catalyzes highly thermodynamically constrained reaction[28] ($\Delta G^{\circ\prime}$ = +25.0 kJ/mol for C4 metabolism). The unchanged expression level of acetyl-CoA C-acetyltransferase suggests that this step functions as a strict thermodynamic bottleneck, where additional enzyme investment cannot meaningfully increase flux[28]. In contrast, enoyl-CoA hydratase (Enzyme 31 in Fig. 3a), the only other enzyme in the RBO cycle that catalyzes a thermodynamically unfavorable reaction (Enzyme 31 in Fig. 3a, $\Delta G^{\circ\prime}$ = +3.3 kJ/mol, for C4 metabolism), was 5.9-fold more abundant in co-culture compared to monoculture (Fig. 3a), suggesting increased thermodynamic pressure on chain elongation. Meanwhile, the terminal enzyme CoA-transferase (Enzyme 34 in Fig. 3a) did not exhibit a significant difference between monoculture and co-culture. The increased ratio of RBO cycle enzymes to the terminal enzyme under co-culture condition reflects an expression profile that promotes greater RBO cycle iterations per product,

`

consistent with the elevated production of C6 and C8 (Fig. 2d).

Kinetic analysis elucidates the role of cross-feeding intermediates in driving chain elongation

Given the central role of lactate as a cross-feeding intermediate, we conducted a kinetic experiment on the co-culture of *N*. sp. FC1 and *M. hexanoica* to assess whether lactate is transiently accumulated or consistently depleted. Lactate was not detected at any point during the 10-day incubation, indicating that it is not only the main driver of chain elongation but also the principal limiting metabolite in lignocellulose-to-MCFA conversion. We propose that this persistent lactate scarcity triggered increased chain elongation in the co-culture condition[29], supported by the observed increase in RBO enzyme expression. This proteome allocation shift is consistent with a compensatory strategy in which cells upregulate enzyme abundance to maintain metabolic flux under substrate-limited conditions[30].

We also found that another cross-feeding metabolite, acetate, governed the MCFAs production kinetics in co-culture conditions. The dynamics of MCFAs production by *M. hexanoica*, which actively consumed acetate during chain elongation, were decoupled from those of fungal growth and metabolite release. The accumulated headspace pressure, which correlates with fungal proliferation and lactate/acetate production, increased rapidly in the first five days (Supplementary Fig. 3)[31]. However, the MCFAs production pattern of *M. hexanoica* was progressively distributed with longer-chain MCFAs increasingly produced during the latter half of the incubation (Fig. 4a, 4c). In contrast, chain elongation kinetics of *P. alactolyticus*, which did not assimilate acetate, closely resembled the kinetics of fungal proliferation and assumed lactate production (Fig. 4b, 4c). These dynamics imply that *P. alactolyticus* operates under pseudo-first-order kinetics on lactate during lactate-scarcity, with

`

chain elongation flux responding directly to transient substrate supply from fungal metabolism. Together, these findings suggest that acetate utilization capacity may play an important role in shaping the temporal organization of chain elongation dynamics in cross-feeding systems.

Techno-economic analysis suggests cost and yield benchmarks for scalable fungal-bacterial CBP systems

Technoeconomic analysis was performed to validate the potential of anaerobic fungal-bacterial consortia as a profitable biorefinery platform and outline design criteria to achieve its practical implementation. This analysis was conducted using the open-source TEA platform BioSTEAM[32] and parameterized based on prior experiments and simple assumptions (Supplementary Note 2, Supplementary Table 3). The model comprises media preparation, fermentation, separation, and distillation (Fig. 5a). An initial analysis, based on experimental results and unoptimized conditions from this study, revealed economic infeasibility. This primarily arose from the high medium cost per product ($127.1 USD/kg_MCFAs), with cysteine (49.7 %), yeast extract (39.4 %), and buffering agents (carbonate and phosphate buffer, 9.5 %) accounting for the majority of expenses (Fig. 5b). The low MCFA titer further increased the cost per product, as the fixed medium cost was allocated across a smaller yield, which is constrained by the low lignocellulose loading (10 g/L) and MCFA yield (0.1 g_MCFAs/g_grass). Sensitivity analysis evaluated the influence of key process design criteria on IRR (Fig. 5c) and utility cost (Fig. 5d), with medium cost, MCFAs yield, and RCG input emerging as the most influential factors. Therefore, we analyzed profitability across different medium costs and MCFA yields (Fig. 5e and 5f for hexanoate and octanoate, respectively) under higher lignocellulose loading (100 g/L) to

`

propose economically feasible engineering design criteria. The results suggest economically feasible targets for medium cost and MCFA yield, represented by the internal rate of return (IRR) contour lines (from left to right, representing IRR levels of 0.1, 0.15, and 0.2, respectively; see Fig. 5e and 5f). Overall, minimizing medium costs and intensifying the process play a crucial role in transitioning this early-stage bioprocess into a scalable and economically viable biomanufacturing system.

Discussion

This study demonstrated fungal-bacterial synthetic consortia as a promising and economically viable platform for direct lignocellulose-to-MCFAs bioconversion. As part of this effort, we isolated a new high-lactate-producing anaerobic fungus, *Neocallimastix* sp. FC1. The optimal co-culture identified here, consisting of *N*. sp. FC1 and *M. hexanoica*, contained the top-performing fungal and bacterial isolates identified in monoculture. This finding suggests that in bottom-up microbial consortia assembly, particularly within systems of relatively low complexity, securing high-performing strains is critical for maximizing productivity in this bioconversion platform, which could be accelerated through culturomics. As the first member in the division of labor, *N*. sp. FC1 expressed CAZymes with multiple catalytic domains and CBMs, forming cellulosome architectures optimized for complex lignocellulose breakdown. Lignocellulose-to-MCFAs conversion was facilitated by cross-feeding of D-lactate and acetate between anaerobic fungi and chain-elongating bacteria. These metabolites played distinct metabolic roles: lactate functioned as the primary fuel for chain elongation, driving flux through the RBO cycle, whereas acetate modulated the timing of product formation, with its involvement associated with delayed synthesis of hexanoate and octanoate. Notably, hexanoate and octanoate were preferentially produced under the lactate scarce conditions,

`

indicating that maintaining low lactate level while maximizing RBO flux can boost lignocellulose-to-MCFA productivity. This shift in product profile is also advantageous from an industrial perspective, as hexanoate and octanoate have higher market value and lower water solubility than butyrate, improving overall process economics[22]. Furthermore, acetate, another cross-feeding intermediate, is a relatively oxidized substrate; thus, limiting its contribution to chain elongation can further enhance the production of longer-chain fatty acids, which are more reduced products[28]. These findings highlight the importance of securing homo-lactic acid fungi to ensure consistent lactate supply while minimizing acetate input that may otherwise divert carbon away from MCFAs.

It is intriguing that the chain elongating bacteria under lactate-scarce co-culture conditions shifted their product profile toward hexanoate and octanoate, fatty acids that require additional elongation steps and impose a greater enzymatic burden on the cells compared to butyrate[28]. In co-culture systems, lactate (the carbon and electron donor for RBO) was rapidly depleted, suggesting that lactate demand by chain elongators outpaced supply by the anaerobic fungus and further constrained bacterial growth. Moreover, upregulation of RBO enzymes in the *M. hexanoica* proteome under co-culture cultivation points to growth limitation in chain-elongating bacteria, as reduced growth is known to trigger a redistribution of proteomic resources away from biosynthetic functions and toward energy-conserving pathways in other systems[33]. Production of more reduced fermentation end-products under growth-limited conditions has been observed in other anaerobic systems as well. For instance, *Clostridium acetobutylicum* transitioned from acidogenesis to solventogenesis as cell growth declined after the exponential phase in batch cultivation[34], and *Clostridium autoethanogenum* shifted from acetate to ethanol production under CO-limited chemostat conditions at higher biomass densities[35]. This pattern may reflect a metabolic adaptation of anaerobic microbes under growth-limited conditions to rebalance surplus electrons due to lower anabolic demand

`

by channeling them into more reduced fermentation end-products.

The technoeconomic analysis further supports the viability of this platform for industrial applications. However, realizing its full economic potential will require strategic advances across three key domains: medium cost reduction, metabolic optimization, and process intensification. The unique ability of anaerobic fungi to deconstruct lignocellulosic biomass without extensive pretreatment or enzymatic hydrolysis enables high solid loadings[36], offering a practical strategy to medium cost reduction and process intensification. Additional cost savings can be achieved by replacing expensive medium components such as cysteine, buffer salts, and yeast extract with renewable alternatives or intensifying microbial cross-feeding[37,38]. Metabolic optimization strategies, such as enhancing lactate production through hydrogenosomal regulation[9,36], refining MCFA selectivity in chain-elongating bacteria[39], and expanding functional guilds (e.g., homoacetogens, ethanol-based chain elongators)[40], could significantly boost productivity and carbon efficiency. For example, incorporating homoacetogens and ethanol-based chain elongators increases the theoretical maximum MCFA yields of hexanoate and octanoate from 27.3 and 25.5 % (yellow vertical dashed line in Fig. 5e, 5f) to 41.0 and 38.2 % (the upper bound of x-axis in Fig. 5e, 5f), respectively. Lastly, process intensification approaches, including high-solids continuous-flow culturing[41,42], solid-state fermentation[43], and membrane-based extraction technologies[22], offer promising routes to improve volumetric productivity and mitigate product inhibition. Advancing this bioprocess toward real-world implementation will require a holistic strategy that integrates microbiome engineering, metabolic engineering, and bioprocess development which could be accelerated by a Design-Build-Test-Learn framework[44]. Building on this foundation, system-level optimization of fungal-bacterial consortia could drive the emergence of next-generation platforms for sustainable biomanufacturing.

`

Materials and methods

Strains and routine cultivation

In this study, two anaerobic fungal strains previously isolated in earlier experiments (*Neocallimastix camerooni* var. constans[45], and *Caecomyces churrovis*[14]) and newly isolated strain (*Neocallimastix* sp. FC1) were used. Isolation, cryopreservation, and subsequent revival of the fungal strains were performed following established protocols for anaerobic gut fungi[46]. *Neocallimastix* sp. FC1 was obtained from lignocellulose-degrading enrichment culture derived from a cow fecal sample[23]. Fungal strains were first revived in 160 mL serum bottles containing 50 mL MC medium supplemented with 10 g/L of milled reed canary grass (1 mm particle size). They were then routinely subcultured every 3 days in M2 medium supplemented with chloramphenicol (100 mg/L) and reed canary grass (10 g/L), using Hungate tubes with a 1 mL inoculum and a 10 mL working volume. Reed canary grass was provided by the U.S. Department of Agriculture, Agricultural Research Service, U.S. Dairy Forage Research Center[16].

Lactate-utilizing chain elongating bacterial strains (*Caproicibacter fermentans* DSM 107079, *Caproiciproducens* sp. 7D4C2 DSM 110548, *Clostridium luticellarii* DSM 29923, *Pseudramibacter alactolyticus* DSM 3980, *Megasphaera cerevisiae* DSM 20461, *Megasphaera elsdenii* DSM20460, and *Megasphaera hexanoica* DSM 106893) were purchased from the German Collection of Micro-organisms and Cell Cultures (DSMZ). Bacterial cultures were revived in ATCC 2107 medium supplemented with sodium lactate (10 g/L) but without soluble starch and dextrose. They were subcultured under the same condition after 4 days of cultivation, by transferring 0.02 mL of preculture into Hungate tubes with 10 mL working volume. For both fungal and bacterial cultures, bottles and tubes

`

were prepared and sealed within a glovebox to maintain strict anaerobic conditions prior to autoclaving. Inoculated cultures were subsequently incubated at 39 °C in a water bath.

Genomic DNA extraction, sequencing, and genome annotation of *Neocallimastix* sp. FC1

Fungal cell mats of *Neocallimastix* sp. FC1 were harvested after four days of growth on sorghum in three different media: MC, M2, and M2 supplemented with 1 g/L yeast extract. The samples were shipped on dry ice to the Arizona Genome Institute for genomic DNA and total RNA extraction. High-quality genomic DNA was extracted at the Arizona Genomics Institute using a modified cetyl trimethylammonium bromide (CTAB) protocol[47]. Briefly, the frozen fungal biomass was cryo-ground using mortar and pestle with liquid nitrogen and subjected to extraction with CTAB buffer for 1 hour at 50 °C. After centrifugation, the supernatant was purified by two repeated extractions with chloroform-isoamyl alcohol (24:1). The upper aqueous phase was recovered and mixed with 3 M sodium acetate (10 % v/v), and genomic DNA was precipitated with isopropanol. The DNA pellet was collected by centrifugation, washed with 70 % ethanol, air-dried for 20 minutes, and dissolved in Tris-EDTA buffer (10 mM Tris, pH 8, 1 mM EDTA) at room temperature followed by RNAse treatment. Subsequently, DNA purity was assessed with a NanoDrop spectrophotometer, concentration was measured with the Qubit HS kit (Invitrogen), and size was validated with the Femto Pulse System (Agilent). The purified genomic DNA of *Neocallimastix* sp. FC1 was shipped to the Joint Genome Institute (JGI) for sequencing and annotation.

For genome sequencing, 1500 ng of genomic DNA was sheared to approximately 10 kb using either a Megaruptor® 3 (Diagenode) or a g-TUBE (Covaris). The sheared DNA was first treated with exonuclease to remove single-stranded ends, followed by DNA damage repair, end-repair, and A-tailing using reagents from the SMRTbell Express Template Prep

`

Kit 2.0 (PacBio). Barcoded overhang adapters from the SMRTbell® Barcoded Adapter Plate 3.0 (PacBio) were then ligated to the prepared DNA fragments, and the resulting libraries were purified using AMPure® PB Beads (PacBio). The purified libraries were pooled based on the required number of reads perd sample to ensure sufficient sequencing coverage. Pooled libraries were size selected using 0.75 % agarose gel cassettes with Marker S1 and the High Pass protocol on a BluePippin system (Sage Science). A sequencing primer was annealed to the SMRTbell templates, and the polymerase was bound using the Sequel II Binding Kit 2.0 (PacBio). Sequencing was performed on a PacBio Sequel IIe platform using SMRT Link v10.2, 8M v1 SMRT cells, and Sequel II Sequencing Kit v2.0, with 1×1800 sequencing movie run times. Circular consensus sequencing (CCS) reads were filtered to remove artifacts and assembled using Flye v2.9-b1768 in HiFi mode[48]. The resulting draft genome was polished using two iterations of Racon v1.4.13 and annotated through the JGI annotation pipeline using assembled transcriptome data[49].

Total RNA extraction, sequencing, and transcriptome assembly of *Neocallimastix* sp. FC1

Total RNA was extracted at the Arizona Genomics Institute using the Qiagen RNeasy® Mini Kit, following the manufacturer's protocol described in the RNeasy® Mini Handbook under the section "Purification of total RNA from plant cells and tissues and filamentous fungi". An on-column DNase digestion step was included to remove residual genomic DNA. Fungal cells were lysed by grinding in liquid nitrogen, and homogenization was performed using a QIAshredder. RNA was eluted in 50 μL of RNase-free water, then re-applied to the column to concentrate the final RNA solution. RNA concentrations exceeded 25 ng/μL as measured by the Invitrogen Qubit 2.0 fluorometer. Integrity was assessed using either the Agilent 2200

`

TapeStation or 2100 Bioanalyzer, with all samples showing RIN or RINe scores above 7. The purified total RNA from *Neocallimastix* sp. FC1 was then shipped to the Joint Genome Institute (JGI) for sequencing and assembly.

For Illumina RNA-Seq, mRNA was isolated from an input of 1000 ng of total RNA with oligo dT magnetic beads and fragmented to 300 bp - 400 bp with divalent cations at a high temperature. Using TruSeq stranded mRNA kit (Illumina), the fragmented mRNA was reverse transcribed to create the first strand of cDNA with random hexamers and SuperScript™ II Reverse Transcriptase (Thermo Fisher Scientific) followed by second strand synthesis. The double stranded cDNA fragments were treated with A-tailing, ligation with NEXTFLEX UDI Barcodes (PerkinElmer) and enriched using 8 cycles of PCR. The prepared libraries were quantified using KAPA Biosystems' next-generation sequencing library qPCR kit and run on a Roche LightCycler 480 real-time PCR instrument. Sequencing of the flow cell was performed on the Illumina NovaSeq sequencer using NovaSeq XP V1.5 reagent kits, S4 flowcell, following a 2x151 indexed run recipe. RNA-Seq reads were filtered and trimmed for quality and contamination using BBDuk (https://sourceforge.net/projects/bbmap/) and assembled using Trinity v2.12.0[50].

For PacBio Iso-Seq, 500 ng of total RNA was used to synthesize full-length cDNA and enriched using 12-20 cycles of PCR with NEBNext® Single Cell/Low Input cDNA Synthesis & Amplification Module (New England BioLabs). The amplified cDNA was purified (or size-selected) with AMPure® PB Beads (PacBio). Libraries were pooled based on the required amount of reads per sample, ensuring each sample received adequate coverage for analysis. The pooled libraries were treated with DNA damage repair enzyme mix, end-repair/A-tailing mix and ligated with barcoded overhang adapters from SMRTbell Barcoded Adapter Plate 3.0 (PacBio) using SMRTbell Express Template Prep Kit 2.0

`

(PacBio). PacBio Sequencing primer was then annealed to the SMRTbell template library and sequencing polymerase was bound to them using Sequel II Binding kit 2.0. The prepared SMRTbell template libraries were then sequenced on a Pacific Biosystems' Sequel IIe sequencer using SMRT Link 12.0, 8M v1 SMRT cells, and Version 2.0 sequencing chemistry with 1x1800 sequencing movie run times. Polished Circular Consensus Sequence (CCS reads) were produced from Pacbio subreads using pbccs v. 4 (ccs --min-passes 3 --min-snr 4 --max-length 21000 --min-length 10 --min-rq 0.98) as described in the official PacBio Iso-Seq analysis pipeline (https://github.com/PacificBiosciences/IsoSeq), classified as full length based on 5' and 3' primers and polyA tail, trimmed for polyA tails, and clustered all the full length CCS reads to produce a single consensus sequence per cluster, following the Iso-Seq protocol[51].

Screening and kinetics experiments

To identify optimal fungal-bacterial pairs for MCFA production, we conducted screening experiments of monocultures and co-cultures using a M2 medium supplemented with 10 g/L (1 %) milled reed canary grass (1 mm particle size). Fungal monocultures were grown for 7 days with 100 mg/L chloramphenicol, with the incubation period determined based on a preliminary kinetic experiment (Supplementary Fig. 3). Bacterial monocultures were subsequently assessed under the same medium condition without chloramphenicol, but with additional supplementation of yeast extract, lactate, and acetate (1, 1.8, and 2.6 g/L, respectively) to support growth and mimic the metabolite profile produced by *N.* sp. FC1 in monoculture. Co-cultures were cultivated in the same medium with 1 g/L of yeast extract but without lactate and acetate to test direct conversion of reed canary grass into MCFAs. All cultures were grown in Hungate tubes with 10 mL working volume, and all experiments

`

were conducted in biological triplicate. For inoculation, 0.1 mL of fungal preculture and 0.01 mL of bacterial preculture were transferred into each tube. The optimal fungal-bacterial combination was selected based on the resulting MCFAs concentration. To further assess the temporal dynamics of metabolite production, a kinetic experiment was performed using co-cultures of *N*. sp. FC1 with either *M. hexanoica* or *P. alactolyticus*. Time-course sampling was conducted destructively by harvesting three biological replicates per condition at each timepoint.

Analytical methods

Headspace pressure and composition were analyzed to evaluate fungal proliferation. Headspace pressure was first measured using a pressure gauge (98766-89, Traceable). Gas composition was analyzed by gas chromatography equipped with a thermal conductivity detector (HP 5890, Hewlett Packard) and CTR I column (Alltech). Helium gas was used as the carrier gas. An isothermal method was applied with 50 °C oven temperature and 10 mins of run time.

All liquid samples were filtered through a 0.22 µm membrane filter and stored at -20 °C before further analysis. Samples were thawed, centrifuged at 10,000 × g for 5 mins, and diluted using HPLC grade water prior to the analysis. Lactate and formate concentrations were quantified using high-performance liquid chromatography (ICS5000 Dionex, Thermo Scientific) with a UV-detector and Aminex HPX-87H column (Bio-Rad). The column was maintained at 50 °C. The mobile phase consisted of 5 mM sulfuric acid, and elution was performed at a flow rate of 0.6 mL/min. Data acquisition and analysis were carried out using Chromeleon 7 software (Thermo). For volatile fatty acids (acetate, propionate, butyrate, pentanoate, hexanoate, heptanoate, and octanoate) quantification, samples were acidified by

`

adjusting formate concentration to 100 mM and were analyzed using gas chromatography (8900 GC System, Agilent) equipped with a mass spectrometry (7000D Triple Quadrupole MS, Agilent) and DB-FatWax column (Agilent). Helium gas was used as the carrier gas with 1 mL/min flow rate, and oven temperature gradient was set as follows: 80 °C for 1 min, a 20 °C/min ramp until 210 °C, 20 °C/min until 250 °C and finally held for 5 mins. The mass spectrometer was operated in dynamic multiple reaction monitoring (dMRM) mode. Target analytes were ionized and fragmented by electron ionization, and the precursor and product ions of target analytes were selected using Agilent software (MassHunter Optimizer, Agilent).

Carbon mass balance experiments and conversion efficiency calculation

Carbon mass balance experiments were conducted under three conditions: (1) uninoculated control, (2) *N*. sp. FC1 monoculture, and (3) co-culture of *N*. sp. FC1 and *M. hexanoica*. All conditions were prepared in five biological replicates using Hungate tubes with a 10 mL working volume of M2 medium supplemented with reed canary grass (10 g/L) and yeast extract (1 g/L). Inoculated cultures were incubated for 7 days prior to mass balance analysis. Samples were analyzed for solid, aqueous, and gas fractions. Headspace pressure and gas composition was analyzed to quantify gaseous carbon dioxide. The entire culture content was then filtered using a vacuum filtration apparatus with a pre-weighed 0.22 μm membrane filter to separate the solid and liquid phases. The liquid fraction was collected in a 50 mL Falcon tube, while the solid retained on the filter was dried at 105°C and weighed to determine the dry solid mass. Carbon content of the solid fraction was further analyzed via elemental analysis (Flash 2000, Thermo Scientific). The liquid fraction was analyzed for organic acid (i.e., lactate, formate and volatile fatty acids) concentrations. In addition, total organic carbon (TOC) and inorganic carbon (IC) were quantified using a TOC analyzer

`

(TOC-L, Shimadzu). Lignocellulose-to-product conversion yield of *N*. sp. FC1 was calculated by dividing the total grams of carbon in fungal fermentation products (lactate, acetate, and formate) by the grams of carbon in the supplemented reed canary grass. The lignocellulose-to-MCFA conversion efficiency of co-cultures was calculated by dividing the total grams of MCFA carbon (hexanoate and octanoate) by the grams of carbon in the supplemented reed canary grass.

Proteomics sample preparation and analysis

Proteomic samples were collected from both monoculture and co-culture conditions. There are three sources of protein in this experiment, which are *N*. sp. FC1, *M. hexanoica*, and grass used as the substrate. Sorghum was selected as an alternative lignocellulosic substrate for proteomic experiments due to the availability of fully annotated genome, which is necessary for the identification of potential plant-derived proteins. To validate the substitution of reed canary grass with sorghum, we compared fermentation kinetics and metabolite profiles of cultures grown on sorghum and reed canary grass under both monoculture and co-culture conditions. Fungal monocultures and fungal-bacterial co-cultures were inoculated in Hungate tubes with a 10 mL working volume of M2 medium supplemented with sorghum (10 g/L) and yeast extract (1 g/L). Bacterial monocultures were inoculated in the same condition but also supplemented with lactate, and acetate (1.8, and 2.6 g/L, respectively). No significant differences were observed in fermentation trends and yields between experiments using reed canary grass and those using sorghum (Supplementary Fig. 4). Particularly, *N*. sp. FC1 rapidly produced its fermentation products within the first 5 days (Supplementary Fig. 4a), and the co-culture of *N*. sp. FC1 and *M. hexanoica* showed higher hexanoate and octanoate production compared to the *M. hexanoica* monoculture (Supplementary Fig. 4d). To

`

minimize disruption of plant cell walls and release of sorghum proteins, cell lysis was performed using bead beating instead of cryo-grinding, resulting in sorghum-derived peptides comprising less than 0.1% of total spectra.

Biomass was harvested during the mid-exponential growth phase. Four fungal monocultures and three fungal-bacterial co-cultures were sampled after 60 h of incubation, while 12 bacterial monocultures were collected after 36 h. Solid samples were obtained by centrifugation, washed once with phosphate buffer saline (pH 7.0), and flash-frozen with liquid nitrogen. Cell lysis, protein isolation, and digestion were performed using procedures outlined by Chirania et al.[52], with minor modifications. Briefly, biomass was lysed by bead beating using 0.15 mm zirconium oxide beads in Tris-HCl buffer (100 mM, pH 8.0) containing 4% sodium dodecyl sulfate and 10 mM DL-Dithiothreitol. Lysates were cleared by centrifugation at 21,000 × g for 10 min and heated at 90 °C for 10 min to denature proteins. Cysteine residues were blocked by alkylation with 30 mM iodoacetamide in the dark for 20 min at room temperature. Proteins were purified by chloroform-methanol extraction, washed with methanol, air-dried, and resolubilized in ammonium bicarbonate (ABC) buffer (100 mM, pH 8.0) containing 4% sodium deoxycholate (SDC). For bacterial monoculture samples, proteins from four tubes were pooled during resolubilization to ensure sufficient protein yield for downstream analysis, generating triplicate samples. Protein concentrations were determined using the BCA assay, and 250 μg of each protein sample was concentrated using 3 kDa MWCO centrifugal filters, rinsed with ABC buffer, and digested with MS-grade trypsin (1:75 w/w) overnight at room temperature, with an additional 3 h digestion after fresh trypsin addition. Tryptic peptides were recovered by filtering through 10 kDa MWCO centrifugal filters. The remaining SDC was removed by formic acid precipitation and water-saturated ethyl acetate extraction. Lastly, peptide samples were dried in a SpeedVac and resuspended in 0.5% formic acid.

`

Peptide separation, detection, and raw mass spectra data processing were performed as previously described by Gois et al.[28], with minor modifications. Peptide samples were loaded onto an EASY-nano LC 1000 system coupled to a Q-Exactive Orbitrap mass spectrometer (Thermo Scientific) and separated on a custom-packed SilicaTip emitter column (New Objective) using ReproSil-Pur C18-AQ resin (Dr. Maisch GmbH). Two solvent solutions comprised 0.1% formic acid in water (Solvent A) and 0.1% formic acid in acetonitrile (Solvent B) delivered at a constant flow rate of 250 nL/min. Chromatographic separation was achieved using the following linear gradient: 0 to 5 min 0% B, increase to 10% B; 5 to 93 min, increase to 40% B; 93 to 95 min, ramp to 95% B; held at 95% B until 105 min; returned to 0% B by 106 min and held until 120 min for column re-equilibration. The mass spectrometer was operated in positive ionization mode with a spray voltage of 3 kV and maintaining the capillary at 275 °C. Full MS scans were collected across a mass-to-charge range of 400-2,000 m/z at a resolution of 70,000 (automatic gain control target: 1e6; max injection time: 30 ms). For tandem mass spectrometry (MS/MS) acquisition, a Top10 data-dependent method was employed and selected the ten most abundant precursor ions within a 0.4 m/z isolation window. MS2 scans were acquired at a resolution of 17,500 (normalized collision energy: 27; max injection time: 50 ms).

Tandem mass spectra were processed with Global Proteome Machine pipeline (GPM; thegpm.org) pipeline (version 2020.11.12.1) and searched with X! Tandem (version X! Tandem Aspartate 2020.11.12.1) against custom protein databases for Sorghum, *N*. sp. FC1 and *M. hexanoica*. To construct a database, the genome assembly of *M. hexanoica* (GCF_012843505.1; ASM1284350v1) was annotated using Prokka (v1.14.6) and eggNOG-mapper (emapper v2.1.12, eggNOG database v5.0.2). The resulting genome annotation files are provided as Supplementary dataset 2. Database searches were performed with fixed carbamidomethylation (cysteine, selenocysteine) and variable modifications allowing for N-

`

terminal pyro-glutamate formation (from glutamine, glutamic acid), N-terminal ammonia loss, deamidation (asparagine, glutamine), and oxidation or dioxidation events on methionine and tryptophan residues. Peptide and protein identifications were validated with Scaffold (v5.1.2, Proteome Software Inc.), using thresholds of greater than 95% probability for peptides and greater than 99% probability for proteins, with a requirement for at least two unique peptides. Protein probabilities were assigned by the Protein Prophet algorithm, while proteins containing shared peptides that could not be uniquely distinguished by MS/MS were grouped according to the principle of parsimony. Quantification was performed using the Top3 total ion current (TIC) approach, and spectral counts for fungal and bacterial proteins were normalized separately by scaling each organism's total spectra within a sample to the average total spectra across all samples. Statistical significance was assessed using t-tests corrected with the Benjamini-Hochberg method. Additionally, identified CAZyme proteins were annotated using dbCAN3 (HMMER-based annotation against CAZy family profiles) and InterProScan (v5.75-106.0) to predict catalytic domains and carbohydrate-binding modules (CBMs).

Technoeconomic analysis

Techno-economic analysis (TEA) was performed using BioSTEAM[32], an open-source Python platform for process simulation and cost estimation. This analysis aimed to assess whether fungal-bacterial co-cultures for direct conversion of reed canary grass into MCFAs could achieve economic viability and to identify key process parameters required for scale-up. The process configuration included four main stages: media preparation, fermentation, product separation, and distillation. BioSTEAM was used to simulate mass and energy flows for each unit operation, coupled with equipment design and cost algorithms to estimate capital and

`

operating costs. Detailed assumptions, parameters, and sensitivity analyses are provided in Supplementary Note 2 and Supplementary Table 3.

Data availability

The *Neocallimastix* sp. FC1 genome assembly and annotation are available from JGI MycoCosm portal [48] (https://mycocosm.jgi.doe.gov/NeoFC1_1) and have been deposited at DDBJ/EMBL/GenBank under the accession XXXXXXXXX [TO BE PROVIDED UPON PUBLICATION]. The mass spectrometry proteomics data have been deposited to the ProteomeXchange Consortium via the PRIDE partner repository with the dataset identifier [TO BE PROVIDED UPON PUBLICATION].

Code availability

All codes used for techno-economic analysis of the lignocellulose-to-MCFAs conversion by fungal-bacterial consortia are available on Github (https://github.com/BK419/Technoeconomic_analysis_lignocellulose_to_MCFAs_fungal_bacterial_co-culture).

Acknowledgements

We acknowledge funding support from the Department of Energy (DOE), Office of Science (DE-SC0022142), the Institute for Collaborative Biotechnologies and National Science Foundation (2128271). This work was also funded by the DOE Joint BioEnergy Institute (http://www.jbei.org) supported by the Office of Biological and Environmental Research of

`

the DOE Office of Science through contract DE-AC02–05CH11231 between Lawrence Berkeley National Laboratory. We further acknowledge support from the Natural Sciences and Engineering Research Council of Canada (RGPIN-2021-02684, NSERC-CREATE 528163-201). The work (proposal: 10.46936/10.25585/60000510) conducted by the U.S. Department of Energy Joint Genome Institute (https://ror.org/04xm1d337), a DOE Office of Science User Facility, is supported by the Office of Science of the U.S. Department of Energy operated under Contract No. DE-AC02-05CH11231. We sincerely thank Dr. Cameron Strachan (University of Veterinary Medicine Vienna) for generously performing the genome annotation of *Megasphaera hexanoica* and providing guidance on annotation processing.

Figure Legend

Figure 1. Schematic diagram of engineering fungal-bacterial synthetic consortia for direct lignocellulose to medium-chain fatty acid (MCFA) conversion.

The top panel illustrates natural rumen microbiome, degrading lignocellulose through a consortium of microbes, with anaerobic fungi acting as key specialists. Their rhizoidal networks and carbohydrate-active enzymes (CAZymes) enable efficient deconstruction of lignocellulosic biomass. Fermentable sugars liberated by fungal and bacterial activities are further metabolized into short-chain fatty acids (SCFAs), CH_4, and CO_2. The bottom panel illustrates a bottom-up microbiome engineering strategy assembling selected fungal and bacterial candidates to redesign collaborative functions within a rationally constructed synthetic microbial consortium. Anaerobic fungi produce lactate and acetate, which are subsequently converted by chain-elongating bacteria into MCFA through reverse β-oxidation (RBO) pathway. Screening of fungal and bacterial candidates identified the co-culture combination with the highest MCFA productivity.

`

Figure 2. Screening determines an optimal fungal-bacterial co-culture and reveals higher medium-chain fatty acid (MCFA) selectivity in co-cultures than in monocultures.

a, Screening of fungal monocultures for lignocellulosic biomass degradation into primary fermentation products. Three fungal isolates were tested: *Caecomyces churrovis* (CC), *Neocallimastix* sp. FC1 (FC1), and *Neocallimastix camerooni* var. constans (NC). **b**, Screening of bacterial monocultures of seven lactate-utilizing, chain-elongating strains for lactate/acetate-to-MCFA conversion. Strains tested were *Caproiciproducens* sp. 7D4C2 (C7), *Caproicibacter fermentens* (CF), *Clostridium luticellarii* (CL), *Megasphaera cerevisiae* (MC), *Megasphaera elsdenii* (ME), *Megasphaera hexanoica* (MH), and *Pseudoramibacter alactolyticus* (PA). Yellow and sky-blue dotted lines indicate initial concentrations of lactate and acetate, respectively. **c**, Screening of fungal-bacterial co-cultures to evaluate direct lignocellulose-to-MCFA conversion. Combinations are denoted as "Fungus-Bacterium" (e.g., FC1-MH). **d**, Average number of reverse β-oxidation (RBO) cycles required for product formation in ME, MH, and PA monocultures and co-cultures with FC1. Butyrate, hexanoate, and octanoate production correspond to one, two, and three RBO cycles, respectively. **e**, Carbon mass balance for Blank (uninoculated control), FC1, and FC1-MH. Screening data (**a**-**d**) are shown as means of biological triplicates (error bars indicate standard deviations). Carbon mass balance data (**e**) are shown as means of biological pentaplicates.

Figure 3. Differential proteomics comparing monoculture and co-culture of *Neocallimastix* sp. FC1 and *Megasphaera hexanoica*.

`

a, Integrated metabolic pathway map and differential proteomics of *N*. sp. FC1 (top orange box) and *M. hexanoica* (bottom purple box). Each reaction is accompanied by paired TIC (Top 3 Total Ion Current value) boxes indicating the average of scaled enzyme abundance in monoculture (left) and co-culture (right). For enzymatic steps with multiple detected proteins, only the one with the highest top 3 TIC value was visualized, and the total number of proteins corresponding to that step is indicated in parentheses (light orange for *N*. sp. FC1, light purple for *M. hexanoica*). The color of each TIC box reflects enzyme abundance, normalized to the highest top 3 TIC value observed within each organism: monoculture malic enzyme (enzyme 17) for *N*. sp. FC1 and co-culture enoyl-CoA hydratase (enzyme 31) for *M. hexanoica*. Reactions that were significantly upregulated in co-culture (FDR < 0.05) are marked with red arrows, and a red star symbol is placed next to the corresponding TIC boxes. **b**, Top 3 TIC values of carbohydrate-active enzyme (CAZyme) and scaffoldin proteins in *N*. sp. FC1 monoculture. CAZymes with identical domains in the same order are shown in bold, with the number in parentheses indicating the number of proteins sharing that domain architecture. Proteins were classified according to their predicted target substrates (i.e., glucan, xylan, pectin, mannan, fructan, chitin, scaffoldin). Data represent the average of biological quadruplicate, with error bars indicating standard deviations.

Figure 4. Kinetic analysis of fungal-bacterial co-cultures demonstrates tight lactate cross-feeding and differences in chain elongation dynamics depending on acetate involvement.

a-b, Kinetics of lignocellulose-to-product conversion in co-cultures of *Neocallimastix* sp. FC1 with *M. hexanoica* (**a**) and *P. alactolyticus* (**b**). **c**, Contribution of each product during the day 5-10 relative to total production in co-cultures of *Neocallimastix* sp. FC1 with *M.*

`

hexanoica or *P. alactolyticus*. All data represent the average of biological triplicates, with error bars indicating standard deviations.

Figure 5. Techno-economic analysis of a fungal-bacterial CBP system for lignocellulose-to-MCFA conversion.

a, Process flow diagram of the fungal-bacterial CBP system for lignocellulose-to-MCFA conversion, including media preparation, fermentation, separation, and distillation. **b**, Pie chart showing the relative cost contribution of medium components for bioreactor cultivation. **c-d**, Sensitivity analysis identifying key process parameters influencing economic performance, measured by internal rate of return (IRR, **c**) and utility cost (**d**). **e-f**, Simulated IRR as a function of medium cost (y-axis) and MCFA yield (x-axis) for hexanoic acid (e) and octanoic acid (f) production. Red dashed contours represent IRR thresholds (0.1, 0.15, 0.2). A yellow vertical dashed line marks the theoretical maximum MCFA yield for a two-member co-culture of an anaerobic fungus and a chain elongating bacterium. The x-axis upper bound corresponds to the theoretical maximum MCFA yield under a CO_2 recovery scenario in which homoacetogens and ethanol-utilizing chain elongating bacteria are added to the synthetic consortium.

`

References

1. Vogt, E. T. C. & Weckhuysen, B. M. The refinery of the future. *Nature* **629**, 295–306 (2024).

2. Lynd, L. R. *et al.* Toward low-cost biological and hybrid biological/catalytic conversion of cellulosic biomass to fuels. *Energy Environ. Sci.* **15**, 938–990 (2022).

3. Minty, J. J. *et al.* Design and characterization of synthetic fungal-bacterial consortia for direct production of isobutanol from cellulosic biomass. *Proc. Natl. Acad. Sci.* **110**, 14592–14597 (2013).

4. Shahab, R. L. *et al.* A heterogeneous microbial consortium producing short-chain fatty acids from lignocellulose. *Science* **369**, eabb1214 (2020).

5. Tsoi, R. *et al.* Metabolic division of labor in microbial systems. *Proc. Natl. Acad. Sci.* **115**, 2526–2531 (2018).

6. Peng, X. *et al.* Genomic and functional analyses of fungal and bacterial consortia that enable lignocellulose breakdown in goat gut microbiomes. *Nat. Microbiol.* **6**, 499–511 (2021).

7. Haitjema, C. H. *et al.* A parts list for fungal cellulosomes revealed by comparative genomics. *Nat. Microbiol.* **2**, 1–8 (2017).

8. Solomon, K. V. *et al.* Early-branching gut fungi possess a large, comprehensive array of biomass-degrading enzymes. *Science* **351**, 1192–1195 (2016).

9. Hooker, C. A., Lee, K. Z. & Solomon, K. V. Leveraging anaerobic fungi for biotechnology. *Curr. Opin. Biotechnol.* **59**, 103–110 (2019).

10. Lankiewicz Thomas S., Lillington Stephen P., & O'Malley Michelle A. Enzyme discovery in anaerobic fungi (*Neocallimastigomycetes*) enables lignocellulosic biorefinery innovation. *Microbiol. Mol. Biol. Rev.* **86**, e00041-22 (2022).

11. Lankiewicz, T. S. *et al.* Lignin deconstruction by anaerobic fungi. *Nat. Microbiol.* **8**, 596 (2023).

12. Mountfort, D. *Anaerobic Fungi: Biology: Ecology, and Function*. (CRC Press, 2020).

13. Swift, C. L., Brown, J. L., Seppälä, S. & O'Malley, M. A. Co-cultivation of the anaerobic fungus *Anaeromyces robustus* with *Methanobacterium bryantii* enhances transcription of carbohydrate active enzymes. *J. Ind. Microbiol. Biotechnol.* **46**, 1427–1433 (2019).

14. Brown, J. L. *et al.* Co□cultivation of the anaerobic fungus *Caecomyces churrovis* with *Methanobacterium bryantii* enhances transcription of carbohydrate binding modules, dockerins, and pyruvate formate lyases on specific substrates. *Biotechnol. Biofuels* **14**, 234 (2021).

15. Li, Y. *et al.* Interactions between anaerobic fungi and methanogens in the rumen and their biotechnological potential in biogas production from lignocellulosic materials. *Microorganisms* **9**, 190 (2021).

16. Brown, J. L. *et al.* Co□cultivation of anaerobic fungi with *Clostridium acetobutylicum* bolsters butyrate and butanol production from cellulose and lignocellulose. *J. Ind. Microbiol. Biotechnol.* **49**, kuac024 (2022).

17. Hillman, E. T. *et al.* Hydrolysis of lignocellulose by anaerobic fungi produces free sugars and organic acids for two-stage fine chemical production with *Kluyveromyces marxianus*. *Biotechnol. Prog.* **37**, e3172 (2021).

18. Seid, N., Ochsenreither, K. & Neumann, A. Caproate production from Enset fiber in one-pot two-step fermentation using anaerobic fungi (*Neocallimastix cameroonii* strain G341) and *Clostridium kluyveri* DSM 555. *Microb. Cell Factories* **22**, 216 (2023).

19. Agena, E. *et al.* Evaluating the feasibility of medium-chain oleochemical synthesis using microbial chain elongation. *J. Ind. Microbiol. Biotechnol.* **51**, kuae027 (2024).

`

20. Angenent, L. T. *et al.* Chain elongation with reactor microbiomes: open-culture biotechnology to produce biochemicals. *Environ. Sci. Technol.* **50**, 2796–2810 (2016).

21. Lu, C. & Weusthuis, R. A. Microbial production of medium-chain-length diols: Current stage and perspectives. *Bioresour. Technol.* **435**, 132932 (2025).

22. Xu, J., Guzman, J. J. L. & Angenent, L. T. Direct medium-chain carboxylic acid oil separation from a bioreactor by an electrodialysis/phase separation cell. *Environ. Sci. Technol.* **55**, 634–644 (2021).

23. Lawson, C. E. *et al.* Functional niches of diverse anaerobic fungi and bacteria driving lignocellulose degradation to volatile fatty acids revealed by metatranscriptomics. *In preparation*.

24. Chen, S. *et al.* Big data mining, rational modification, and ancestral sequence reconstruction inferred multiple xylose isomerases for biorefinery. *Sci. Adv.* **9**, eadd8835.

25. Biddy, M. J. *et al.* The techno-economic basis for coproduct manufacturing to enable hydrocarbon fuel production from lignocellulosic biomass. *ACS Sustain. Chem. Eng.* **4**, 3196–3211 (2016).

26. Artzi, L., Bayer, E. A. & Moraïs, S. Cellulosomes: bacterial nanomachines for dismantling plant polysaccharides. *Nat. Rev. Microbiol.* **15**, 83–95 (2017).

27. Couger, M. B., Youssef, N. H., Struchtemeyer, C. G., Liggenstoffer, A. S. & Elshahed, M. S. Transcriptomic analysis of lignocellulosic biomass degradation by the anaerobic fungal isolate *Orpinomyces* sp. strain C1A. *Biotechnol. Biofuels* **8**, 208 (2015).

28. Gois, I. M., Bowers, C. M., Kim, B.-C., Flick, R. & Lawson, C. E. Distinct acetate utilization strategies differentiate butyrate and octanoate producing chain-elongating bacteria. *bioRxiv* 2025.05.02.651941 (2025) doi:10.1101/2025.05.02.651941.

29. Strachan, C. R. *et al.* Distinct lactate utilization strategies drive niche differentiation between two co-existing *Megasphaera species* in the rumen microbiome. *ISME J.* **19**, wraf147 (2025).

30. Flamholz, A., Noor, E., Bar-Even, A., Liebermeister, W. & Milo, R. Glycolytic strategy as a tradeoff between energy yield and protein cost. *Proc. Natl. Acad. Sci.* **110**, 10039–10044 (2013).

31. Theodorou, M. K., Davies, D. R., Nielsen, B. B., Lawrence, M. I. G. & Trinci, A. P. J. Determination of growth of anaerobic fungi on soluble and cellulosic substrates using a pressure transducer. *Microbiology* **141**, 671–678 (1995).

32. Cortes-Peña, Y., Kumar, D., Singh, V. & Guest, J. S. BioSTEAM: A fast and flexible platform for the design, simulation, and techno-economic analysis of biorefineries under uncertainty. *ACS Sustain. Chem. Eng.* **8**, 3302–3310 (2020).

33. Scott, M. & Hwa, T. Shaping bacterial gene expression by physiological and proteome allocation constraints. *Nat. Rev. Microbiol.* **21**, 327–342 (2023).

34. Amador-Noguez Daniel, Brasg Ian A., Feng Xiao-Jiang, Roquet Nathaniel, & Rabinowitz Joshua D. Metabolome remodeling during the acidogenic-solventogenic transition in *Clostridium acetobutylicum*. *Appl. Environ. Microbiol.* **77**, 7984–7997 (2011).

35. Valgepea, K. *et al.* Maintenance of ATP homeostasis triggers metabolic shifts in gas-fermenting acetogens. *Cell Syst.* **4**, 505-515.e5 (2017).

36. Saye, L. M. G. *et al.* The anaerobic fungi: challenges and opportunities for industrial lignocellulosic biofuel production. *Microorganisms* **9**, (2021).

37. He, Q., Hemme, C. L., Jiang, H., He, Z. & Zhou, J. Mechanisms of enhanced cellulosic bioethanol fermentation by co-cultivation of *Clostridium* and *Thermoanaerobacter* spp. *Bioresour. Technol.* **102**, 9586–9592 (2011).

38. Vinzelj, J., Joshi, A., Insam, H. & Podmirseg, S. M. Employing anaerobic fungi in biogas production:

`

challenges & opportunities. *Bioresour. Technol.* **300**, 122687 (2020).

39. Wang, J. & Yin, Y. Biological production of medium-chain carboxylates through chain elongation: An overview. *Biotechnol. Adv.* **55**, 107882 (2022).

40. Kim, B.-C. R., Kleinsteuber, S. & Lawson, C. E. Carbon-efficient waste upcycling: combining syngas fermentation and chain elongation with synthetic consortia. *Curr. Opin. Biotechnol.* **94**, 103321 (2025).

41. Zhu, W.-Y. *et al.* Growth and survival of anaerobic fungi in batch and continuous-flow cultures. *Anaerobe* **2**, 29–37 (1996).

42. Zhu, W.-Y., Theodorou, M. K., Nielsen, B. B. & Trinci, A. P. Dilution rate increases production of plant cell-wall degrading enzymes by anaerobic fungi in continuous-flow culture. *Anaerobe* **3**, 49–59 (1997).

43. Soccol, C. R. *et al.* Recent developments and innovations in solid state fermentation. *Biotechnol. Res. Innov.* **1**, 52–71 (2017).

44. Helleckes, L. M., Hemmerich, J., Wiechert, W., von Lieres, E. & Grünberger, A. Machine learning in bioprocess development: from promise to practice. *Trends Biotechnol.* **41**, 817–835 (2023).

45. Blair, E. M. *et al.* Genomic and transcriptomic characterization of carbohydrate-active enzymes in the anaerobic fungus *Neocallimastix cameroonii* var. constans. *G3 GenesGenomesGenetics* jkaf137 (2025) doi:10.1093/g3journal/jkaf137.

46. Peng, X., Swift, C. L., Theodorou, M. K. & O'Malley, M. A. Methods for genomic characterization and maintenance of anaerobic fungi. in *Fungal Genomics: Methods and Protocols* (eds. de Vries, R. P., Tsang, A. & Grigoriev, I. V.) 53–67 (Springer New York, New York, NY, 2018). doi:10.1007/978-1-4939-7804-5_5.

47. Doyle, J. J. & Doyle, J. L. A rapid DNA isolation procedure for small quantities of fresh leaf tissue. *Phytochem. Bull.* (1987).

48. Kolmogorov, M., Yuan, J., Lin, Y. & Pevzner, P. A. Assembly of long, error-prone reads using repeat graphs. *Nat. Biotechnol.* **37**, 540–546 (2019).

49. Grigoriev, I. V. *et al.* MycoCosm portal: gearing up for 1000 fungal genomes. *Nucleic Acids Res.* **42**, D699–D704 (2014).

50. Grabherr, M. G. *et al.* Full-length transcriptome assembly from RNA-Seq data without a reference genome. *Nat. Biotechnol.* **29**, 644–652 (2011).

51. Wang, B. *et al.* Unveiling the complexity of the maize transcriptome by single-molecule long-read sequencing. *Nat. Commun.* **7**, 11708 (2016).

52. Chirania, P. *et al.* Metaproteomics reveals enzymatic strategies deployed by anaerobic microbiomes to maintain lignocellulose deconstruction at high solids. *Nat. Commun.* **13**, 3870 (2022).

Fig. 1: Synthetic microbiome for direct lignocellulose-to-MCFA conversion

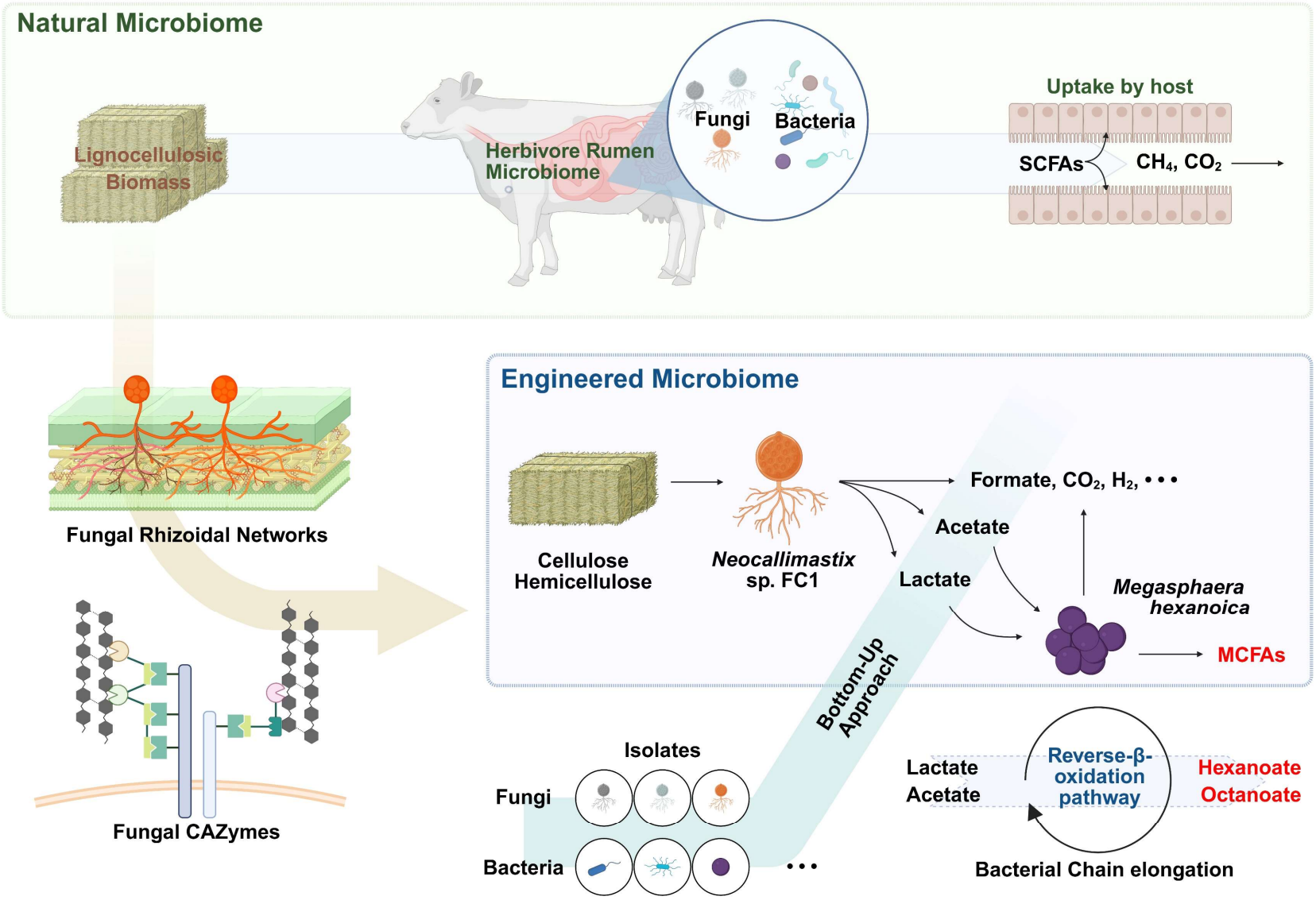

Fig. 2: Screening for optimal fungal-bacterial co-cultures

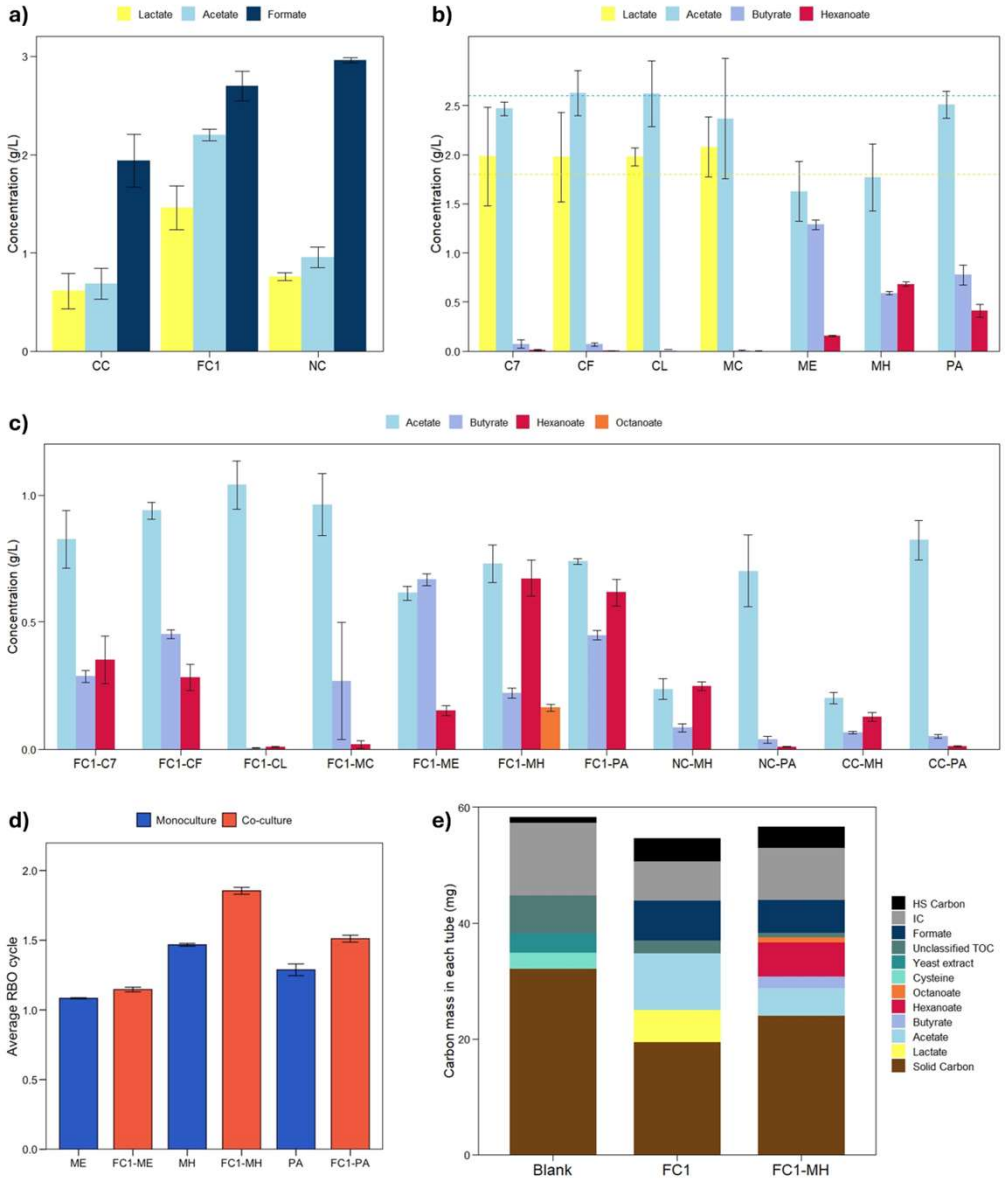

Fig. 3: Fungal and bacterial proteomes

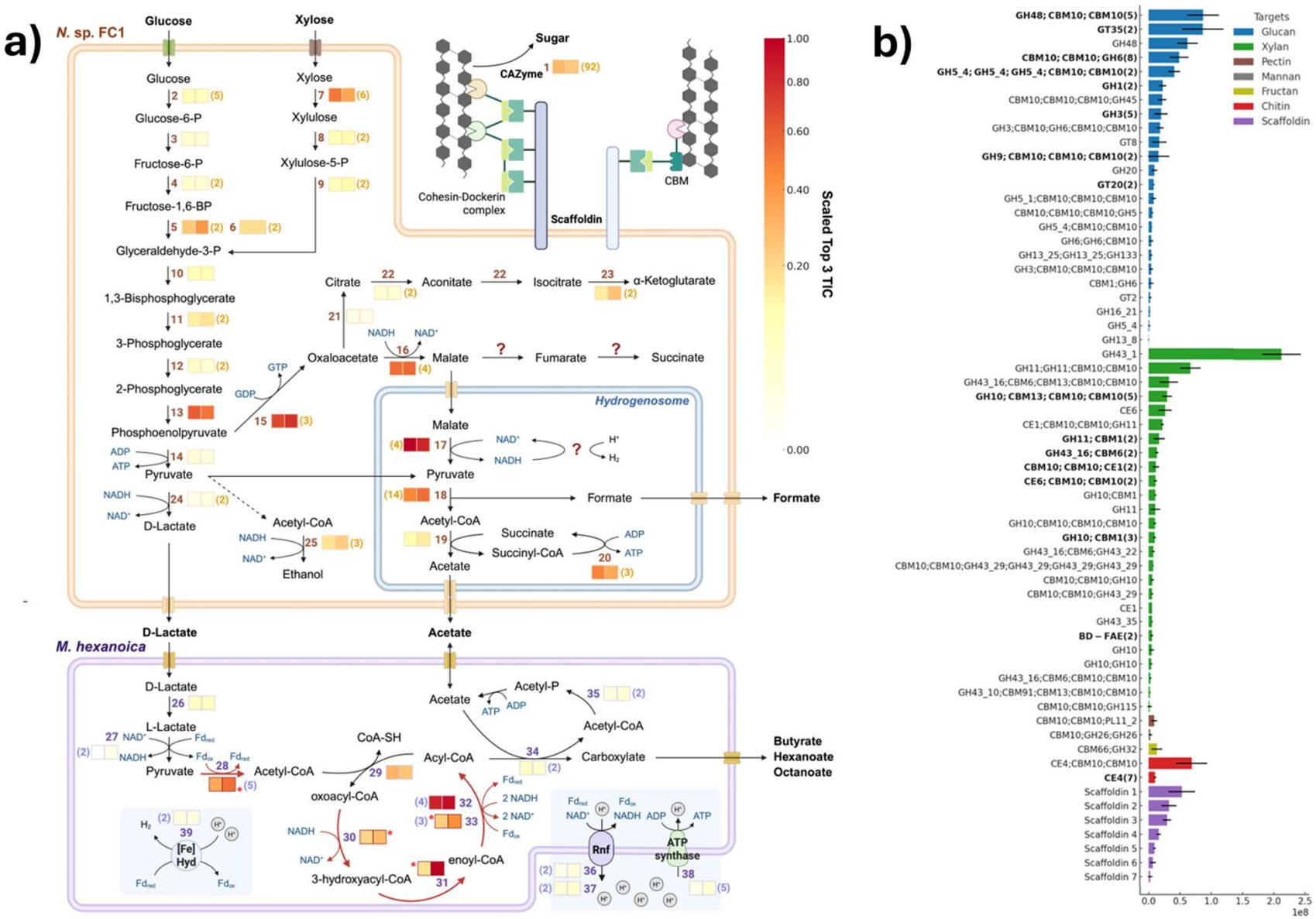

Fig. 4: Chain elongation kinetics

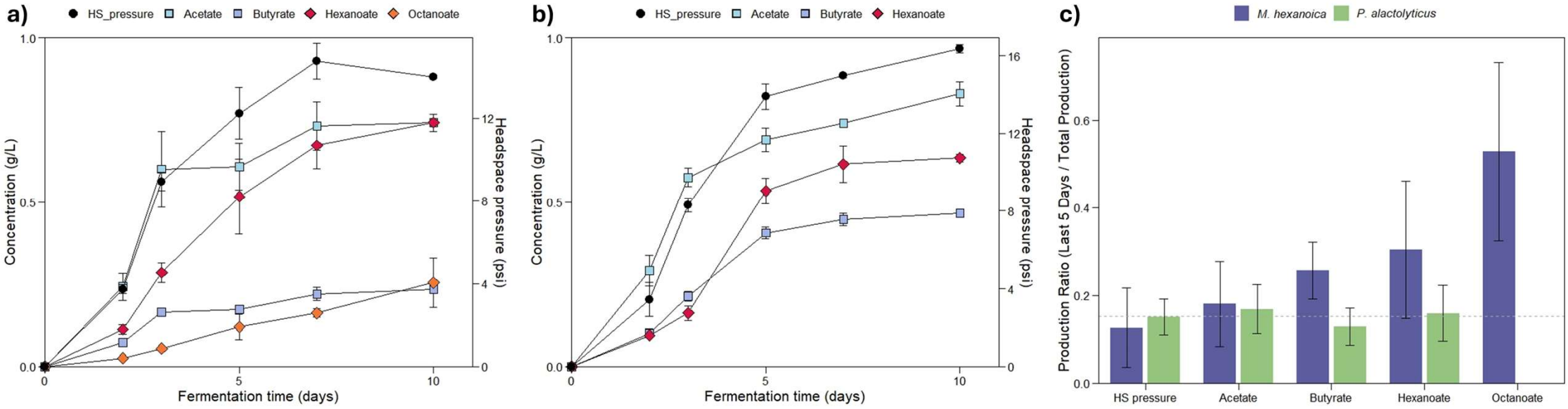
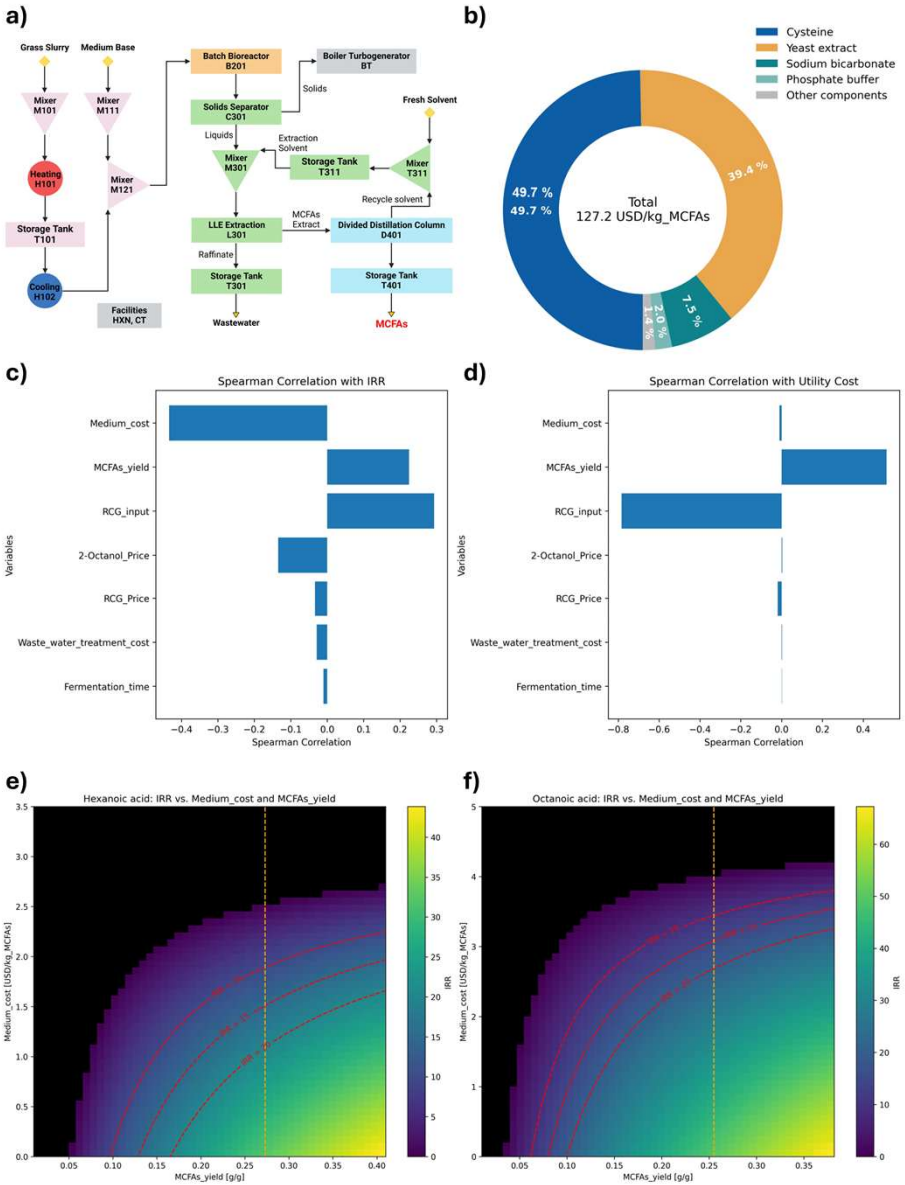
Fig. 5: Techno-economic analysis